US 20090028253A1

(19) **United States**

(12) **Patent Application Publication**

Wu et al.

(10) **Pub. No.: US 2009/0028253 A1**

(43) **Pub. Date: Jan. 29, 2009**

(54) **TONE-INTERLEAVED CODED MODULATION SCHEME FOR MIMO OFDM COMMUNICATION**

(76) Inventors: **Wen-Rong Wu**, Hsinchu City (TW); **Shih-Chi Shen**, Hsinchu City (TW)

Correspondence Address:
KAMRATH & ASSOCIATES P.A.
4825 OLSON MEMORIAL HIGHWAY, SUITE 245
GOLDEN VALLEY, MN 55422 (US)

(21) Appl. No.: **11/782,528**

(22) Filed: **Jul. 24, 2007**

Publication Classification

(51) **Int. Cl.**
H04L 27/28 (2006.01)

(52) **U.S. Cl.** **375/260**

(57) **ABSTRACT**

A MIMO OFDM system for TICM is provided. The tone-level interleaver at the transmitter uses a block of N_T symbols as its basic unit. This results in different decoding architectures at the receiver. The main advantage of TICM is to merge soft-bit demapping into the Viterbi algorithm. Taking the advantage of the trellis structure inherent in the Viterbi algorithm, TICM can have lower computational complexity and potentially better performance than BICM with the LSD detector and the vector demapper. Although the tone-level interleaving may not have spatial diversity gain, the performance is not affected in 802.11n environments.

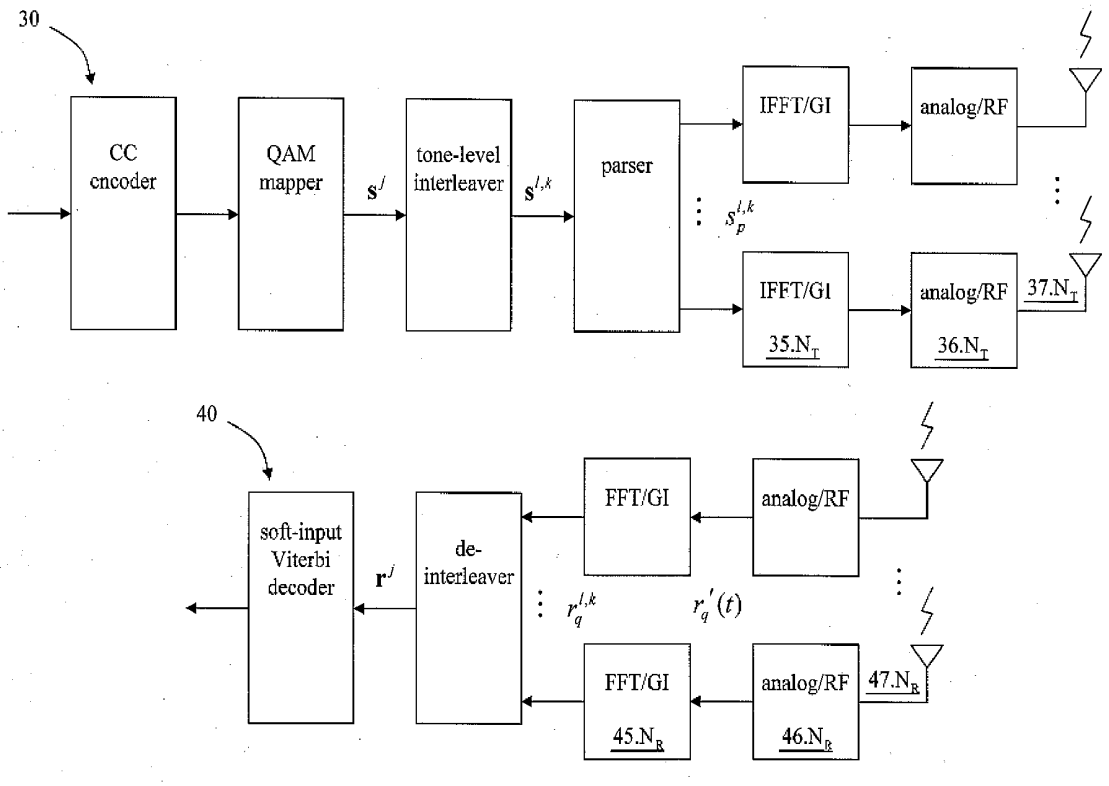

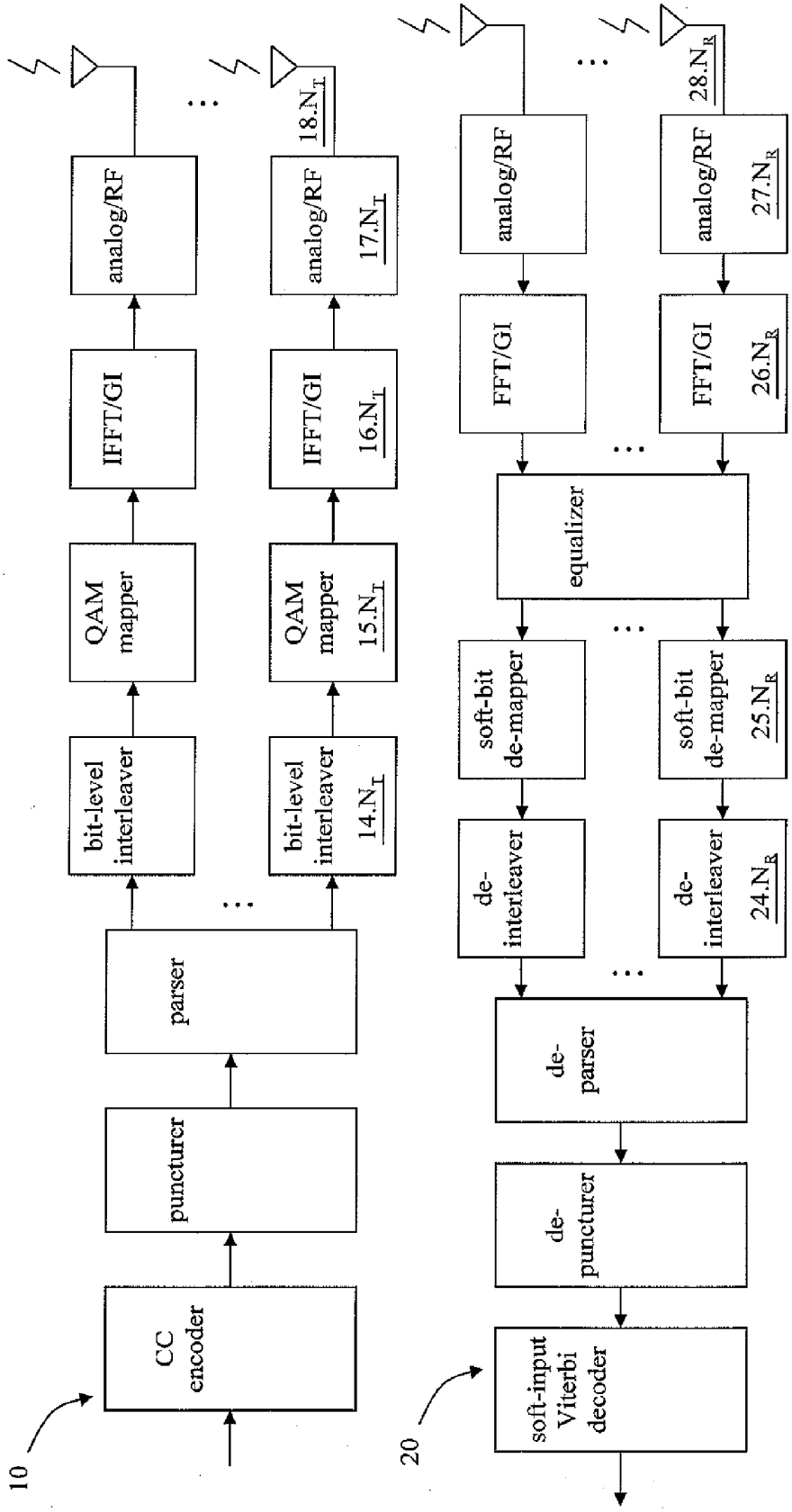

FIG. 1 (CONVENTIONAL ART)

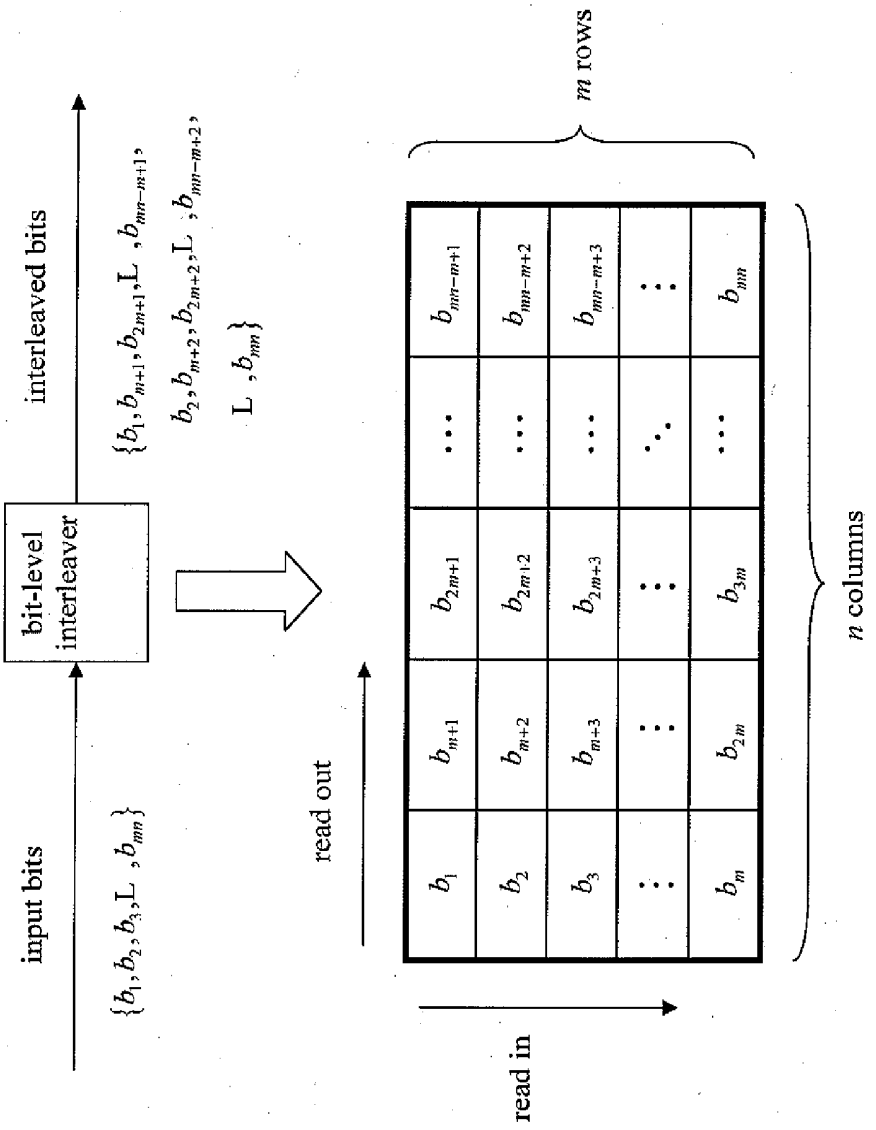

FIG. 2 (CONVENTIONAL ART)

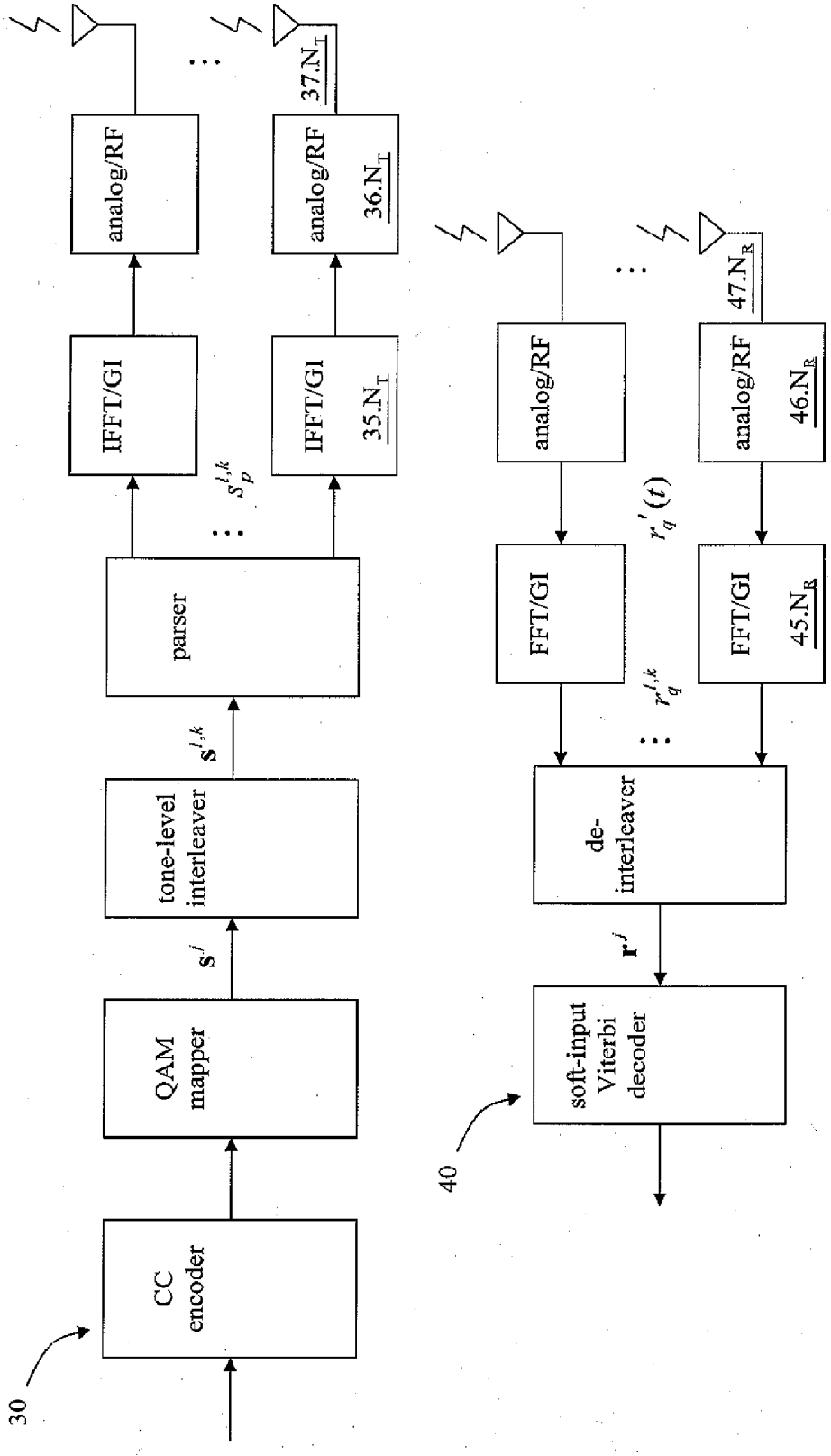
30
CC encoder
QAM mapper
tone-level interleaver
parser
IFFT/GI
IFFT/GI 35.N_T
analog/RF
analog/RF 36.N_T
37.N_T
40
soft-input Viterbi decoder
de-interleaver
FFT/GI
FFT/GI 45.N_R
analog/RF
analog/RF 46.N_R
47.N_R

FIG. 3

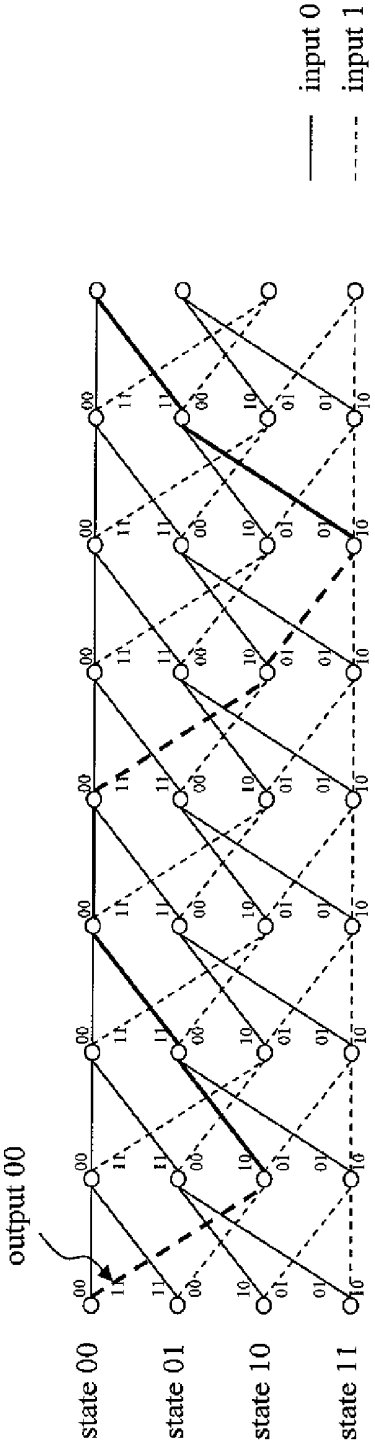
input 0
input 1
output 00
state 00
state 01
state 10
state 11

FIG. 4A

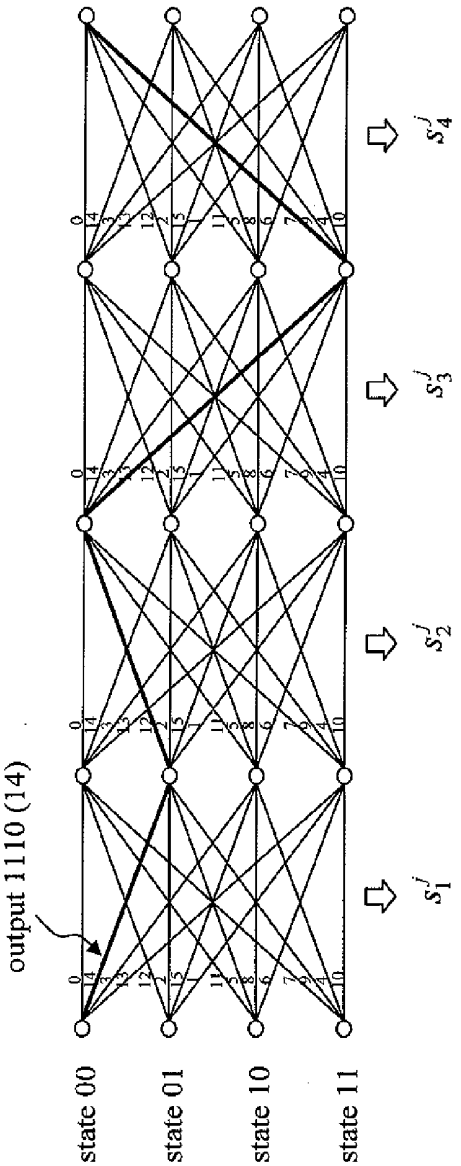
output 1110 (14)
state 00
state 01
state 10
state 11
s_1^j
s_2^j
s_3^j
s_4^j

FIG. 4B

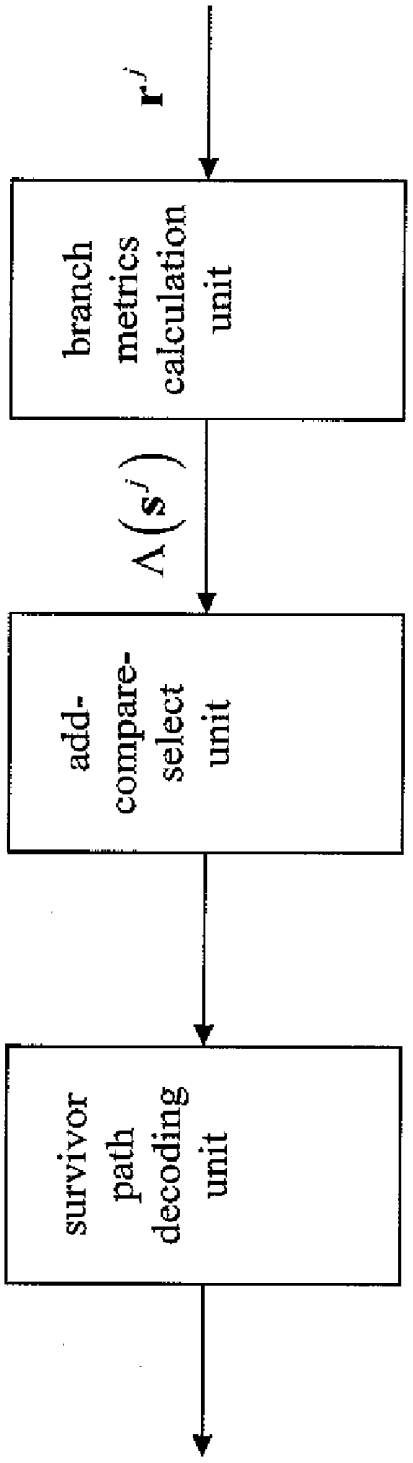
$\mathbf{r}^j$
branch metrics calculation unit
$\Lambda(\mathbf{s}^j)$
add-compare-select unit
survivor path decoding unit

FIG. 5

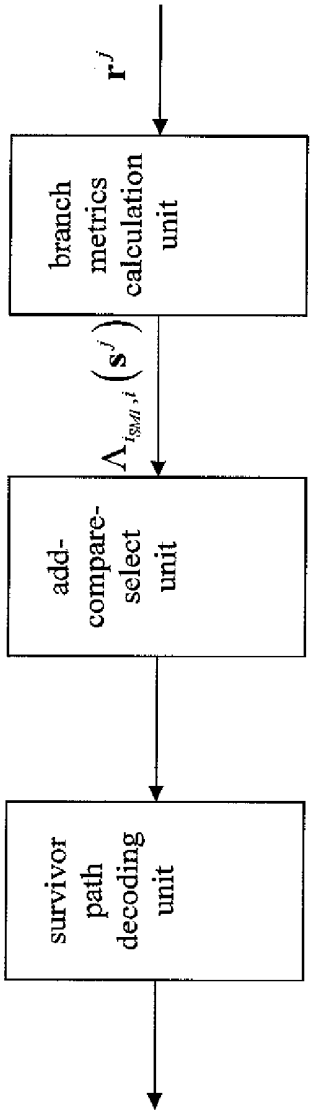
$\mathbf{r}^j$
branch metrics calculation unit
$\Lambda_{i_{SMI},i}\left(\mathbf{s}^j\right)$
add-compare-select unit
survivor path decoding unit

FIG. 6

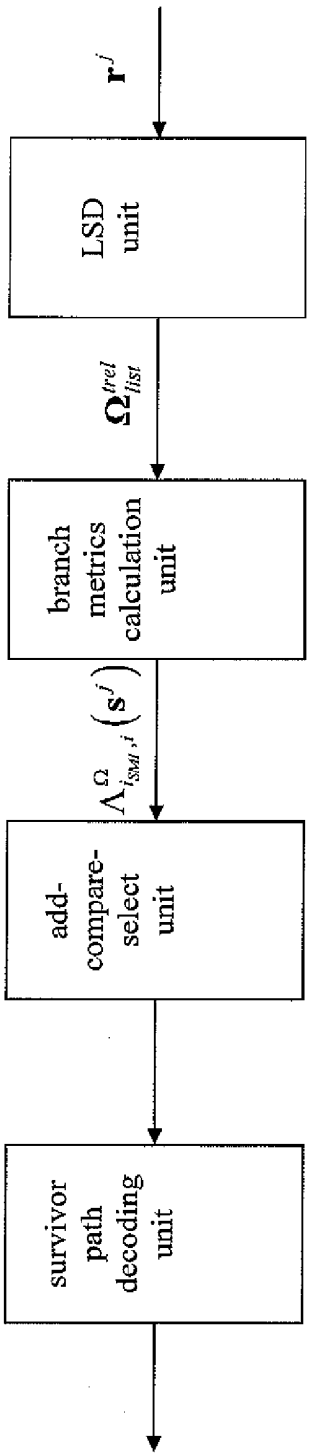
$\mathbf{r}^j$
LSD unit
Ω_{list}^{trel}
branch metrics calculation unit
$\Lambda_{i_{SMI},i}^{\Omega}\left(\mathbf{s}^j\right)$
add-compare-select unit
survivor path decoding unit

FIG. 7

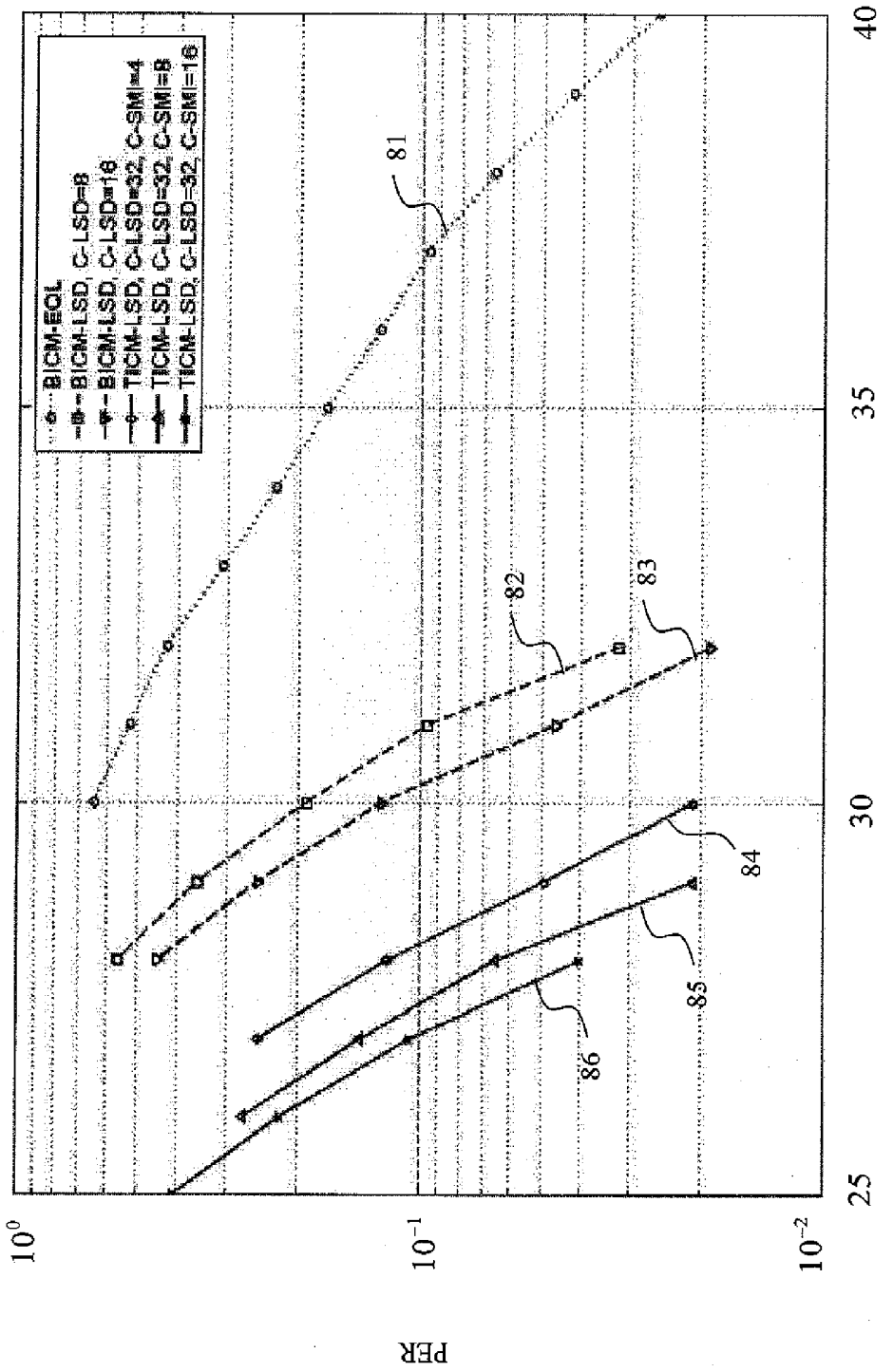
BICM-ECL
BICM-LSD, C-LSD=8
BICM-LSD, C-LSD=16
TICM-LSD, C-LSD=32, C-SMI=4
TICM-LSD, C-LSD=32, C-SMI=8
TICM-LSD, C-LSD=32, C-SMI=16
81
82
83
84
85
86
10^0
10^{-1}
10^{-2}
PER
25
30
35
40
SNR (dB)

FIG. 8

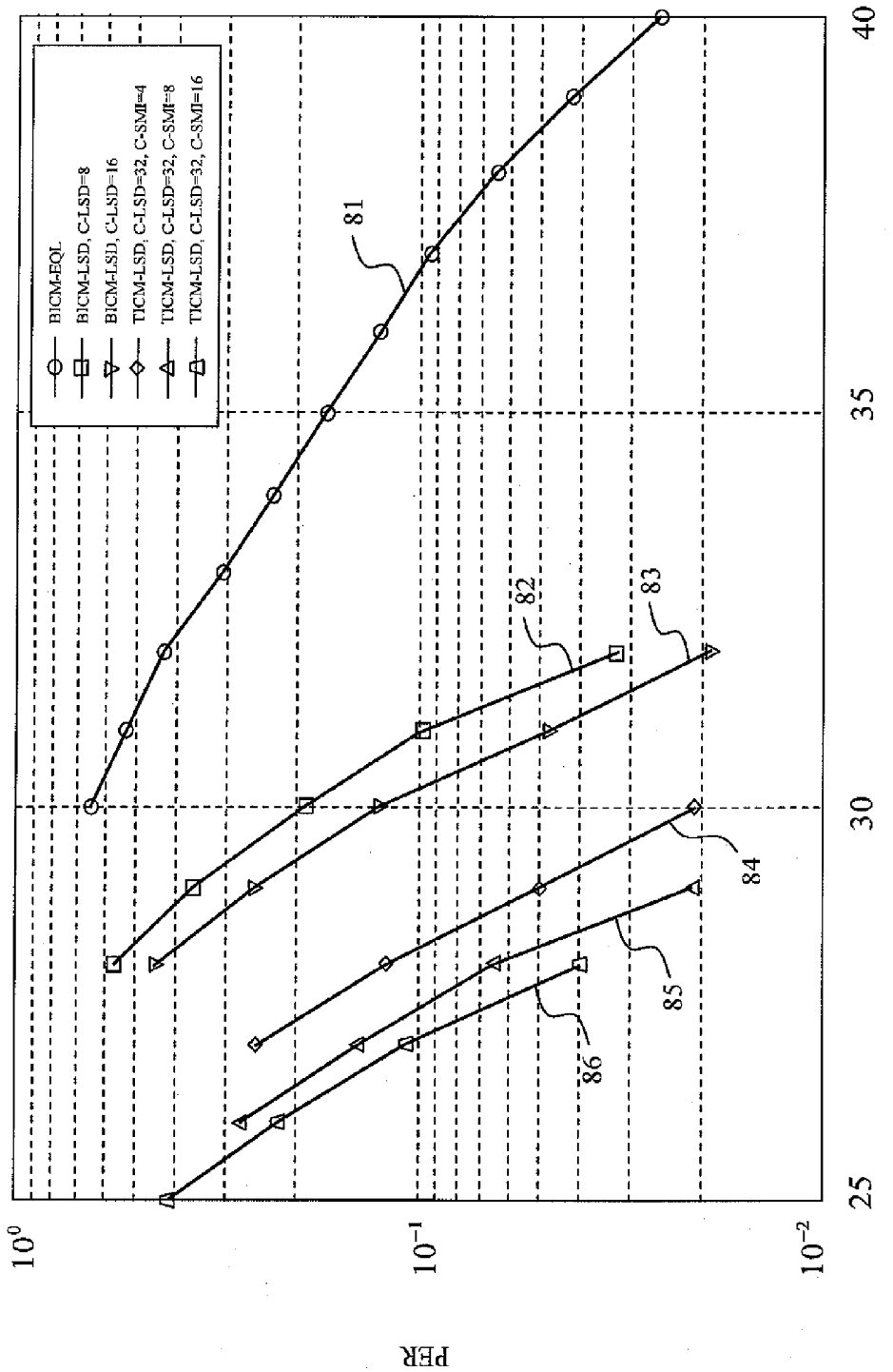
BICM-EQL
BICM-LSD, C-LSD=8
BICM-LSD, C-LSD=16
TICM-LSD, C-LSD=32, C-SMI=4
TICM-LSD, C-LSD=32, C-SMI=8
TICM-LSD, C-LSD=32, C-SMI=16
81
82
83
84
85
86
10^0
10^{-1}
10^{-2}
PER
25
30
35
40
SNR (dB)

FIG. 8

TONE-INTERLEAVED CODED MODULATION SCHEME FOR MIMO OFDM COMMUNICATION

BACKGROUND OF THE INVENTION

[0001] 1. Field of the Invention

[0002] The present invention relates to wireless communications. More particularly, the present invention relates multi-input multi-output (MIMO) orthogonal frequency division multiplexing (OFDM) wireless communications.

[0003] 2. Description of the Prior Art

[0004] Orthogonal frequency division multiplexing (OFDM) technique is known to have high spectrum efficiency, and robust against inter-symbol interference (ISI) and fading caused by multi-path propagation. Another useful technique is bit-interleaved coded modulation (BICM), which has been widely used in OFDM systems. BICM is used between an encoder and a modulator for eliminating burst errors. Due to a fast growth, existing wireless communication systems are not able to meet the demands for transmission bandwidth. Multi-input multi-output (MIMO) technique, by employing multiple transmit and receive antennas, is introduced to provide higher channel capacity which increases approximately linearly with the number of antennas used. Combing with MIMO structure, OFDM systems can further enhance the spectrum efficiency.

[0005] FIG. **1** is a block diagram illustrating a conventional MIMO OFDM system for BICM. Referring to FIG. **1**, the conventional MIMO OFDM system **1** includes a transmitter **10** and a receiver **20**, wherein the transmitter **10** includes N_T transmit antennas **18**.**1**-**18**.N_T, and the receiver **20** includes N_R receive antennas **28**.**1**-**28**.N_R. An MIMO channel is formed among the transmit antennas **18**.**1**-**18**-N_T and the receive antennas **28**.**1**-**28**.N_R.

[0006] At the transmitter **10**, information bits are encoded by a convolutional code (CC) encoder **11**. The coded bits outputted from the CC encoder **11** may be punctured for variable code rates by a puncturer **12**. The coded and punctured bits are parsed to multiple antenna streams by a parser **13** in a round-robin fashion. Each antenna stream is coped with a bit-level interleaver **14**.*p*, a QAM mapper **15**.*p*, a IFFT/GI modulator **16**.*p*, an analog/RF circuit **17**.*p* and a transmit antenna **18**.*p*, where p represents the index of the transmit antenna and $p \in \{1, 2, 3, \ldots, N_T\}$. It is noted that the QAM mapper **15**.*p* and the IFFT/GI modulator **16**.*p* form an OFDM structure.

[0007] The bit-level interleaver **14**.*p* formats its input bits in a rectangular array of m rows and n columns as shown in FIG. **2**. Referring to FIG. **2**, the input bits $\{b_1, b_2, b_3, L, b_{nm}\}$ are read in row-wise and read out column-wise by the bit-level interleaver **14**.*p*. Then, the bit-level interleaver **14**.*p* outputs the interleaved bits $\{b_1, b_{m+1}, b_{2m+1}, L, b_{mn-m+1}, b_2 b_{m+2}, b_{2m+2}, L, b_{nm-m+2}, L, b_{mn}\}$. Referring again to FIG. **1**, the interleaved bits are converted into QAM symbols by the QAM mapper **15**.*p*. The QAM symbols are then fed to the IFFT/GI modulator **16**.*p*, arranged into OFDM symbols, and finally transmitted by the analog/RF circuit **17**.*p*.

[0008] At the receiver **20**, an electromagnetic signal outputted from the transmitter **10** is passed through the MIMO channel and received by the receiver **20**. Simply speaking, the receiver **20** is the reverse process of the transmitter **10**. For example, the IFFT/GI modulator **16**.*p* inserts guard interval (GI) and then implements inverse FFT (IFFT), however, the FFT/GI demodulator **26**.*q* implements FFT and then removes GI, where q represents the index of the receive antenna and $q \in \{1, 2, 3, \ldots, N_R\}$. The bit-level deinterleaver **24**.*q* formats its input bits in the same rectangular array as shown in FIG. **2**, but its input bits are read in column-wise and read out row-wise.

[0009] For the equalizer **29**, the commonly used equalizers include the zero-forcing (ZF) and minimum mean-square error (MMSE) equalizers. After equalization, the MIMO OFDM system **1** in each tone becomes multiple single-input single-output (SISO) systems. For the Viterbi decoder **21**, a one-dimensional soft-bit demapper **25**.*q* for each SISO system is also required. It is conceptually simple and easy to be implemented, but not optimal. This is because that after equalization, noise components at the receive antennas **28**.**1**-**28**.N_R become correlated. Accordingly, the performance of the MIMO OFDM system **1** for BICM can be greatly degraded in typical MIMO channel conditions. A solution to the problem is to apply an optimal multi-dimensional soft-bit demapper. However, its computational complexity is very high.

[0010] Recently, a soft detector using a list sphere decoding (LSD) algorithm, called the LSD detector, has been proposed to replace the equalizer **29**. The LSD detector provides a list of candidates allowing us to compute the bit metrics with lower complexity. Although the LSD detector can reduce the complexity of the optimal multi-dimensional soft-bit demapper, the computational complexity is still high and the size of the memory required to save the candidate list is large particularly when the number of the transmit antennas is large and the size of the QAM mapper is large.

[0011] It would, therefore, be desirable to provide a MIMO OFDM system having lower computational complexity particularly when the number of the transmitter antennas is large and the size of the constellation mapper (e.g. QAM mapper) is large.

SUMMARY OF THE INVENTION

[0012] The present invention provides a MIMO OFDM system using tone-interleaved coded modulation (TICM) scheme to reduce the computational complexity of the decoding process.

[0013] In one aspect of the invention, the MIMO OFDM system includes a transmitter and a receiver, wherein the transmitter includes a channel encoder, a constellation mapper, a tone-level interleaver, a parser and a plurality of multicarrier modulators; and the receiver includes multicarrier demodulators, a tone-level deinterleaver and a channel decoder.

[0014] At the transmitter, the channel encoder receives information bits and outputs coded bits. The constellation mapper converts the coded bits into constellation symbols according to constellation mappings. The tone-level interleaver receives the constellation symbols and using a symbol block of N_T constellation symbols as its basic unit for interleaving, where N_T represents the number of the transmit antennas. The parser parses interleaved symbol blocks and outputs parsed signals to each corresponding transmit antenna. The multicarrier modulators modulate the parsed signals before the parsed signals are transmitted through the corresponding transmit antennas.

[0015] At the receiver, the multicarrier demodulators demodulate received signals passed through a MIMO channel formed by the transmit and receive antennas. The tone-level deinterleaver deinterleaves the received signals after

demodulation and outputs deinterleaved symbol blocks. The channel decoder decodes the deinterleaved symbol blocks. In one embedment, the channel decoder is a Viterbi decoder including a branch metrics calculation unit, an add-compare-select (ACS) unit and a survivor path decoding unit, wherein the branch metrics calculation unit calculates branch metrics according to the deinterleaved symbol blocks and the estimated MIMO channel; the ACS unit performs an ACS operation according to the branch metrics; and the survivor path decoding unit decodes a survived path with maximum likelihood provided by the ACS operation.

[0016] Because the MIMO OFDM system for TICM uses a block of N_T symbols as its basic unit for interleaving, it results in different decoding architectures at the receiver, for example, the soft-bit demapping is merged into the Viterbi decoding. TICM scheme can have lower computational complexity and potentially better performance. To further reduce the complexity of TICM, we make some simplifications and extend the use of the LSD algorithm in the decoding process.

BRIEF DESCRIPTION OF THE DRAWINGS

[0017] The accompanying drawings are included to provide a further understanding of the invention, and are incorporated in and constitute a part of this specification. The drawings illustrate embodiments of the invention and, together with the description, serve to explain the principles of the invention.

[0018] FIG. **1** is a block diagram illustrating a conventional MIMO OFDM system for BICM;

[0019] FIG. **2** is a diagram illustrating a conventional bit-level interleaver formatting its input bits in a rectangular array of m rows and n columns;

[0020] FIG. **3** is a block diagram illustrating a MIMO OFDM system for TICM in accordance with the preferred embodiment of the present invention;

[0021] FIGS. **4**A and **4**B are a trellis diagram at the j^{th} stage for the CC encoder and its re-drawn version respectively;

[0022] FIG. **5** is a block diagram illustrating a Viterbi decoder at the MIMO OFDM receiver for TICM in accordance with the preferred embodiment of the present invention;

[0023] FIG. **6** is a block diagram illustrating an alternative Viterbi decoder at the MIMO OFDM receiver for TICM as shown in FIG. **5**;

[0024] FIG. **7** is a block diagram illustrating another alternative Viterbi decoder at the MIMO OFDM receiver for TICM as shown in FIG. **5**; and

[0025] FIG. **8** is a simulation diagram illustrating the performance comparison of the MIMO OFDM receiver for BICM with a MMSE equalizer, the MIMO OFDM receivers for BICM with an LSD detector and a vector demapper, and the MIMO OFDM receivers for TICM as shown in FIG. **7**.

DESCRIPTION OF THE PREFERRED EMBODIMENTS

[0026] Reference will now be made in detail to the preferred embodiments of the present invention, examples of which are illustrated in the accompanying drawings. Wherever possible, the same reference numbers are used in the drawings and the description to refer to the same or like parts.

[0027] Before the description for the present invention, we define notations to be used in the sequel. Scalars are denoted in lower case letters, vectors are denoted in lower case bold letters, and matrices are denoted in upper case bold letters. Also, $[\bullet]^T$ and $[\bullet]^H$ indicate the transpose and conjugate transpose of a vector or matrix inside the bracket respectively. Now, the MIMO OFDM systems for TICM in accordance with the present invention will be described in three subsections I-III as follows.

I. Transmitter and Receiver in the MIMO OFDM systems for TICM

[0028] FIG. **3** is a block diagram illustrating a MIMO OFDM system for TICM in accordance with the preferred embodiment of the present invention. Referring to FIG. **3**, the MIMO OFDM system **3** includes a transmitter **30** and a receiver **40**. The transmitter **30** includes a channel encoder **31**, a constellation mapper **32**, a tone-level interleaver **33**, a parser **34**, multicarrier modulators **35**.**1**-**35**.N_T, analog/RF circuits **36**.**1**-**36**.N_T and transmit antennas **37**.**1**-**37**.N_T. The receiver **40** includes a channel decoder **41**, a tone-level deinterleaver **43**, multicarrier demodulators **45**.**1**-**45**.N_R, analog/RF circuits **46**.**1**-**46**.N_R and receive antennas **47**.**1**-**47**.N_R.

[0029] In this embodiment, the channel encoder **31** is a CC encoder; and accordingly, the channel decoder **41** is a Viterbi decoder. The constellation mapper **32** is a QAM mapper, and accordingly its output, the constellation symbol, is a QAM symbol. The multicarrier modulator **35**.*p* is an IFFT/GI modulator which first inserts GI and then implements IFFT; and accordingly, the multicarrier demodulator **45**.*q* is a FFT/GI demodulator which first implements FFT and then removes GI. The analog/RF circuit **36**.*p* may include a digital-to-analog converter, an analog RF filter, an amplifier, and so on; and, the analog/RF circuit **46**.*q* may include an amplifier, an analog RF filter, an analog-to-digital converter, and so on.

[0030] The MIMO OFDM system **3** employs multiple transmit and receive antennas for data transmission. An MIMO channel is formed among these transmit and receive antennas. We assume that the MIMO channel in each tone is quasi-static Rayleigh fading, and there are no inter-symbol interference (ISI) and inter-carrier interference (ICI). Thus, the model for the MIMO OFDM system **3** can be represented as

$$r^{l,k}=H^k\cdot s^{l,k}+n^{l,k} \qquad \text{Eq. (1)}$$

where $r^{l,k}=[r_1^{l,k},L,r_q^{l,k},L,r_{N_R}^{l,k}]^T$ represents the received vector signal at the k^{th} tone and the l^{th} OFDM symbol after FFT, where q represents the index of the receive antenna and $q \in \{1, 2, 3, \ldots, N_R\}$;

[0031] $s^{l,k}=[s_1^{l,k},L,s_p^{l,k},L,s_{N_T}^{l,k}]^T$ represents the transmitted vector signal at the k^{th} tone and the l^{th} OFDM symbol before IFFT, where p represents the index of the transmit antenna and $p \in \{1, 2, 3, \ldots, N_T\}$;

$$H^k=\begin{pmatrix} h_{1,1}^k & K & h_{1,N_T}^k \\ M & h_{q,p}^k & M \\ h_{N_R,1}^k & L & h_{N_R,N_T}^k \end{pmatrix}$$

represents the frequency response of the MIMO channel at the k^{th} tone, where the element $\{h_{q,p}^k\}$ represents the coupling between the p^{th} transmit antenna and the q^{th} receive antenna; and

[0032] $n^{l,k}=[n_1^{l,k},L,n_q^{l,k},L,n_{N_R}^{l,k}]^T$ represents the received vector noise, and each element $\{n_q^{l,k}\}$ is an

independent and identically distributed (i.i.d.) complex Gaussian random variable with zero mean and variance $\sigma^2=N_0$.

[0033] At the transmitter **30**, information bits are first convolutionally encoded by the CC encoder **31**, and then the resultant coded bits are converted into QAM symbols by the QAM mapper **32**. The QAM symbols are interleaved by the tone-level interleaver **33**. The parser **34** will parse the transmitted vector signal $s^{l,k}$ to each corresponding transmit antenna **37**.*q*. For example, the parsed signal $\{s_p^{l,k}\}$ called the p^{th} transmitted signal of the transmitted vector signal $s^{l,k}$ before IFFT, is sequentially coped with the corresponding IFFT/GI modulator **35**.*p*, the corresponding analog/RF circuit **36**.*p* and the corresponding transmit antenna **37**.*p*.

[0034] One special feature of the MIMO transmitter for TICM is that the channel encoder (e.g. the CC encoder **31**) and the constellation mapper (e.g. the QAM mapper **32**) can be independently designated without considering the optimum of them. Accordingly, the optimum of the MIMO transmitter for TICM is less than that of the STTC (space time trellis code) transmitter because at the STTC transmitter the channel encoder and the constellation mapper are dependently optimally designated. But, the design of the STTC transmitter is more and more difficult particularly when the number of the transmit antennas is large and the size of the QAM mapper is large.

[0035] The main difference between BICM and TICM lies in the level of interleaving. The bit-level interleaver (e.g. interleaver **14**.*p* as shown in FIG. **1**) uses a bit as its basic unit while the tone-level interleaver (e.g. interleaver **33** as shown in FIG. **3**) uses a block of N_T symbols as its basic unit. The j^{th} block (or called symbol block), $s^j=[s_1^j,s_2^j,L,s_{N_T}^j]^T$, is consisted of N_T modulated symbols, mapped from $N_T \cdot N_{BPSC}$ coded bits where N_{BPSC} represents the number of bits transmitted per sub-channel at a time instant. The index j starts from "1" to "$L_S \cdot K$", where L_S represents the number of OFDM symbols per transmit antenna and K represents the number of OFDM sub-channels. Thus, there are total $L_S \cdot K$ blocks at each transmission package.

[0036] For example, we assume that the CC encoder **31** with $R_C=1/2$ and $K_{CC}=3$ is used, where R_C represents the code rate and K_{CC} represents the constraint length. We also assume that 16-QAM mapper **32** and four transmit antennas **37**.**1**-**37**.**4** are used (i.e. the size of the QAM mapper **32** is 16, and $N_T=4$). Encoding process of the CC encoder **31** can be explained in the trellis diagram as shown in FIG. **4**A. Referring to FIG. **4**A, there are $2^{K_{CC}-1}=4$ possible states. Each state has two incoming and two outgoing branches. A transition from one state to another in response to input (i.e. information bit) "0" is represented by a solid line and that in response to input "1" is represented by a dashed line. The binary number labelled on each branch represents the output (i.e. coded bits) of the CC encoder **31** as it moves from one state to another according to the binary input value. Since a block of four QAM symbols are mapped from sixteen coded bits, we define one stage in the trellis diagram as eight continuous time instants in the trellis diagram. Each stage is also a basic unit in the decoding process at the receiver **40**, which is similar to a radix-2^8 Viterbi structure.

[0037] To explain further, FIG. **4**A can be re-drawn as that in FIG. **4**B if each two consecutive time instants are merged into one. Referring to FIG. **4**B, the decimal number, transformed from the binary number, labelled on each branch, represents the output (i.e. coded bits) of the CC encoder **31** as it moves from one state to another. If the coded bits are assumed to be {11 10, 11 00, 11 01, 01 11} according to FIG. **4**A, accordingly they can be represented as {14, 12, 13, 7} according to FIG. **4**B. Now, each time instant in the trellis outputs four coded bits (e.g. "1110" or 14), and the four coded bits are mapped to a 16-QAM symbol (e.g. s_1^j). Thus, for four transmit antennas, $s^j=[s_1^j,s_2^j,s_3^j,s_4^j]^T$ represents a block of four QAM symbols associated with the outputs of the CC encoder **31** at the j^{th} stage through the trellis diagram.

[0038] At the receiver **20** for BICM, soft-bit values are first computed by the soft-bit demapper **25**.*q*, and these values are then used in the soft-bit Viterbi decoder **21** to calculate the branch metrics (BMs). However, at the receiver **40** for TICM, the BMs can be directly computed without involving the soft-bit demapper.

[0039] Referring again to FIG. **3**, at the receiver **40**, the received vector signal $r^{l,k}$ is deinterleaved by the tone-level deinterleaver **43**, and the resultant deinterleaved block r^j is passed to the soft-bit Viterbi decoder **41**. Referring to FIG. **5**, the Viterbi decoder **41** includes three major units: a branch metrics calculation unit **51**, an add-compare-select (ACS) unit **52** and a survivor path decoding unit **53**. The BMs are calculated by the branch metrics calculation unit **51** according to the deinterleaved block r^j and the estimated MIMO channel through the trellis diagram as shown in FIG. **4**B. As mentioned, the whole trellis as shown in FIG. **4**B corresponds to one stage. The BMs outputted from the branch metrics calculation unit **51** are fed into the ACS unit **52** to select the state with the greatest state metric, wherein the state metric indicates the greatest accumulated BMs among all legal paths. Finally, the survived path is traced back and decoded by the survivor path decoding unit **53**.

[0040] Since the conditional probability density function (p.d.f.) of the deinterleaved block r^j obeys complex Gaussian distribution, the output symbols corresponding to the maximum likelihood path through the trellis diagram can be defined as

$$\Phi^{ML-path} = \underset{\Phi^{trel,j}\in\Psi^{trel,j}}{\operatorname{argmax}} \sum_{j=1}^{L_S\cdot K} \left(-|r^j - \Pi^j \cdot \Phi^{trel,j}|^2\right) \quad \text{Eq. (2)}$$

where $r^j=[r_1^j,L,r_{N_T}^j]^T$ represents the deinterleaved block;

[0041] H^j represents the frequency response of the MIMO channel after deinterleaving;

[0042] $\Phi^{trel,j}=[\phi_1^{trel,j},L,\phi_{N_T}^{trel,j}]^T$ represents the output symbols corresponding to the hypothesized legal path at the j^{th} stage in the trellis diagram, and

[0043] $\Psi^{trel,j}=[\psi_1^{trel,j},L,\psi_{N_T}^{trel,j}]^T$ presents the subset of the output symbols corresponding to all legal paths at the j^{th} stage in the trellis diagram.

Let $N_{IBPS}=N_T \cdot N_{BPSC} \cdot R_C$ be the number of information bits per stage. Thus, finding the maximum likelihood path needs to examine $2^{K_{CC}-1} \cdot (2^{N_{IBPS}})^{L_S \cdot K}$ paths through the trellis diagram, where $2^{K_{CC}-1}$ represents the number of beginning states in the trellis diagram.

[0044] Here we can use the Viterbi algorithm to reduce the complexity. Note that the total trellis stages are $L_S \cdot K$. We define the BM of the block s^j at the j^{th} stage outputted from the branch metrics calculation unit **51** for TICM as

$$\Lambda(s^j)=-|r^j-H^j \cdot \Phi^{trel,j}|^2 \quad \text{Eq. (3)}$$

Then, we define the i^{th} state metric (or called path metric) at the j^{th} stage for TICM as

$$M_i(j), \text{ where } i \in \{1, 2, \ldots, 2^{K_{CC}-1}\} \quad \text{Eq. (4)}$$

The state metric indicates the greatest accumulated BMs among all legal paths from the first stage to the j^{th} stage merging to the i^{th} state. Thus, we can have the recursive equation for state metric as

$$M_i(j+1) = \max_{i' \in I} \{M_{i'}(j) + \Lambda_{i',i}(s^j)\} \quad \text{Eq. (5)}$$

where $\Lambda_{i',i}(s^j)$ represents the BM over the transition branch form the i^{th} state to the i^{th} state at the j^{th} stage, and I represents the subset of all states having permissible transition from the previous stage to the i^{th} state at the j^{th} stage.

[0045] To compute the state metric, the ACS unit **52** will perform the add-compare-select (ACS) operation. The detailed operation is explained below.

[0046] (a) Add: Add new BM to the previous state metric for each path merging to the state.

[0047] (b) Compare: Compare the total metric of different paths merging to the state.

[0048] (c) Select: Select the path with the greatest metric merging to the state and record both the updated state metric and the survived path.

After $M_i(L_S \cdot K+1)$ is evaluated at the $(L_S \cdot K)^{th}$ stage, the state with the greatest state metric is then selected. Then, the survived path is traced back, from the last stage to the first stage, by the survivor path decoding unit **53**. Each detected branch at the j^{th} stage will then output N_{IBPS} information bits. This procedure is called chaining (trace) back. After chaining back, the decoding process is completed.

[0049] Observing equation (3), we find that there are $2^{K_{CC}-1} \cdot 2^{N_{IBPS}}$ legal paths through the trellis diagram at the j^{th} stage. In other words, the complexity for evaluating the BM, $\Lambda(s^j)$, grows exponentially with $K_{CC}+N_{IBPS}$. Obviously, direct implementation of equation (3) may not be feasible. Note that $2^{K_{CC}-1}$ corresponds to the number of beginning states at the j^{th} stage, and $2^{N_{IBPS}}$ corresponds to the number of all legal paths starting from each beginning state. In the following subsections, we will propose suboptimal approaches to reduce the computational complexity. The first one (Subsection II) is to reduce the number of the beginning states, and the second one (Subsection III) is to reduce the number of legal paths being searched.

II. Suboptimal Receiver with State Reduction

[0050] FIG. **6** is a block diagram illustrating an alternative Viterbi decoder at the MIMO OFDM receiver for TICM. Referring to FIG. **6**, the alternative Viterbi decoder **41'** includes a sub-optimal branch metrics calculation unit **61**, the add-compare-select unit **52** and the survivor path decoding unit **53**.

[0051] Since that the BM at each stage for TICM corresponds to a block of N_T symbols, information embedded in the BM is higher than that in BICM (only one bit). Thus, the state metrics in TICM provide more reliable information than that in BICM. Define the subset of beginning states with the greatest C_{SMI} state metrics as I_{SMI}, where $1 \leqq C_{SMI} \leqq 2^{K_{CC}-1}$. With predictable performance degradation, we can only consider the paths beginning from I_{SMI} with higher likelihood and eliminate the others with lower likelihood. Define the i^{th} state belonging to I_{SMI} as i_{SMI}, and the BM of s^j, starting from the i_{SMI}^{th} state and merging to the i^{th} state at the j^{th} stage, as $\Lambda_{i_{SMI},i}(s^j)$. Then, the recursive equation in equation (5) can be modified as

$$M_i(j+1) = \max_{i_{SMI} \in I_{SMI}} \{M_{i_{SMI}}(j) + \Lambda_{i_{SMI},i}(s^j)\} \quad \text{Eq. (6)}$$

[0052] This suboptimal decoding method is almost the same with the receiver above-mentioned in Subsection I. However, the complexity of the BM evaluation is reduced to a factor of $C_{SMI}/2^{K_{CC}-1}$.

[0053] We now use the receiver above-mentioned in Subsection I as an illustration example. Let $C_{SMI}=2$. At the j^{th} decoding stage, suppose that the first and third state have the greatest two state metrics. Then, we only have to evaluate $\Lambda_{1,i}(s^j)$ and $\Lambda_{3,i}(s^j)$, where $i \in \{1, 2, 3, 4\}$. Finally, the ACS module will determine the survived branch. Note that C_{SMI} determines how well equation (6) can approximate equation (5). So, there is a trade off between the computational complexity and performance degradation.

III. Suboptimal Receiver with LSD

[0054] FIG. **7** is a block diagram illustrating another alternative Viterbi decoder at the MIMO OFDM receiver for TICM. Referring to FIG. **7**, the alternative Viterbi decoder **41"** includes an LSD unit **71**, the sub-optimal branch metrics calculation unit **61**, the add-compare-select unit **52** and the survivor path decoding unit **53**.

[0055] Even we have reduced the number of the beginning states, there are still $2^{N_{IBPS}}$ legal paths for each beginning state. The computational complexity for evaluating $\Lambda_{i_{SMI},i}(s^j)$ still grows exponentially with $2^{N_{IBPS}}$. Observe equation (3), we can find that the BM calculation problem is an ML problem. Thus, we can extend the use of the LSD detector to reduce the computational complexity of the BM calculation. With a tree structure formulation, we can exclude the symbols corresponding to the hypothesized legal paths making $|r^j - H^j \cdot \Phi^{trel,j}|^2$ large. In this way, we can search for the legal paths that maximize the term in equation (6). With a suitable number of candidate paths, maximization of equation (6) can be well approximated. Define the subset of the symbol sequences corresponding to the candidate paths as candidate path list, Ω_{list}^{trel}. Note that the legal paths in the LSD unit **71** here $(2^{N_{IBPS}})$ is much smaller than those in BICM $(2^{N_T \cdot N_{BPSC}})$. This is due to the trellis structure we have here. So, the BM of s^j that begins from the i_{SMI}^{th} state at the j^{th} stage within Ω_{list}^{trel} can be represented as

$$\Lambda_{i_{SMI}}^{\Omega}(s^j) = -|r^j - H^j \cdot \Phi^{trel,j}|^2 \quad \text{Eq. (7)}$$

where $\Phi^{trel,j} \in \Psi^{trel,j} \cap \Omega_{list}^{trel}$, and $\Phi^{trel,j}=[\phi_1^{trel,j}, L, \phi_{N_T}^{trel,j}]^T$ represents the output symbols corresponding to the hypothesized legal path starting from the i_{SMI}^{th} state; and

[0056] $\Psi^{trel,j}=[\psi_1^{trel,j}, L, \psi_{N_T}^{trel,j}]^T$ represents the subset of the output symbols corresponding to all legal paths starting from the i_{MI}^{th} state.

Then, equation (6) can be modified as

$$M_i(j+1) = \max_{i_{SMI} \in I_{SMI}} \{M_{i_{SMI}}(j) + \Lambda_{i_{SMI},i}^{\Omega}(s^j)\} \quad \text{Eq. (8)}$$

where $\Lambda_{i_{SMI},i}^{\Omega}(s^j)$ represents the BM over the transition branch form the i_{SMI}^{th} state to the i^{th} state. Thus, to evaluate $\Lambda_{i_{SMI},i}^{\Omega}(s^j)$, the number of the LSD detectors in the LSD unit **71** we

needed is C_{SMI}. We will show that the computational complexity can be greatly reduced with these suboptimal approaches. Referring to the article "Achieving Near-Capacity on a Multiple-Antenna Channel" proposed by B. M. Hochwald and S. ten Brink, the LSD unit **71** only check those points that lie inside a sphere with the given radius r_{LSD}, which is large enough to enclose the term maximizing equation (6) and represented as

$$\sum_{i=1}^{N_T}(u_{i,i})^2\cdot\left|\begin{array}{c}\varphi_{N_T+1-i}^{trel}-y_{N_T+1-i}+\\ \sum_{j=i+1}^{N_T}\frac{u_{i,j}}{u_{i,i}}\cdot(\varphi_{N_T+1-i}^{trel}-y_{N_T+1-i})\end{array}\right|^2\le r_{LSD}^2 \quad \text{Eq. (9)}$$

where $y^j=[y_1,L,y_{N_T}]^T$ represents the equalized vector signal of r^j; and

$$U=\begin{pmatrix}u_{11} & K & u_{1,N_T}\\ M & u_{i,j} & M\\ 0 & L & u_{N_T,N_T}\end{pmatrix},$$

being obtained by using the Cholesky factorization such that

[0057] $U^H\cdot U=H^H\cdot H$, represents an upper triangular matrix with $u_{i,i}$ real and positive. Each term in the summation over i in equation (9) is nonnegative, and the LSD method will build a tree structure. With bounds on $\phi_1^{trel,j},L,\phi_{N_T}^{trel,j}$, the LSD method can eliminate unlikely paths step by step using equation (9).

[0058] The dimension of LSD is defined as N_T since there are N_T elements inside each candidate hypothesis. Then, the decoding process of the LSD unit **71**, starting from the i_{SMI}^{th} state (at the j^{th} stage), can be summarized as follows.

[0059] (a) Start the process from $i=N_T$ and eliminate the rest terms, $i=1,L,N_T-1$, in the summation over i in equation (9). Then, equation (9) can be modified as

$$u_{N_T,N_T}^2\cdot|\phi_1^{trel}-y_1|^2\le r_{LSD}^2 \quad \text{Eq. (10)}$$

The LSD will choose all possible values for ϕ_1^{trel} satisfying equation (10) from ψ_1^{trel}, where ψ_1^{trel} is determined by all branches leaving from the i_{SMI}^{th} state.

[0060] (b) If there is no possible value for ϕ_1^{trel}, back to (a) and enlarge the radius of the sphere. Or choose one of the possible values for ϕ_1^{trel} and take $i=N_T-1$ into consideration. Then, equation (9) can be modified as

$$u_{N_T,N_T}^2\cdot|\varphi_1^{trel}-y_1|^2+ \quad \text{Eq. (11)}$$
$$u_{N_T-1,N_T-1}^2\cdot\left|\varphi_2^{trel}-y_2+\frac{u_{N_T-1,N_T}}{u_{N_T-1,N_T-1}}\cdot(\varphi_1^{trel}-y_1)\right|^2\le r_{LSD}^2\Rightarrow$$
$$\left|\varphi_2^{trel}-y_2+\frac{u_{N_T-1,N_T}}{u_{N_T-1,N_T-1}}\cdot(\varphi_1^{trel}-y_1)\right|^2\le$$
$$\frac{r_{LSD}^2-u_{N_T,N_T}^2\cdot|\varphi_1^{trel}-y_1|^2}{u_{N_T-1,N_T-1}^2}$$

The LSD will choose all possible values for ϕ_2^{trel} satisfying equation (11) from ψ_2^{trel}, where ψ_2^{trel} is determined by the state that ϕ_1^{trel} is going to enter.

[0061] (c) If there is no possible value for ϕ_2^{trel}, back to (b) and choose another possible value for ϕ_1^{trel}. A new subset of all possible values for ϕ_2^{trel} from ψ_2^{trel} will be found. Or choose one of the possible values for ϕ_2^{trel} and take $i=N_T-2$ into consideration.

[0062] (d) Keep the same process running until LSD reaches $\phi_{N_T}^{trel}$. Then, a complete hypothesized transmitted vector signal $\Psi^{trel}=[\psi_1^{trel},L,\psi_{N_T}^{trel}]^T$ will be added into the candidate path list. The same process will be repeated until all candidate hypotheses inside the sphere are added into the candidate pat list.

Similar LSD from all other states belonging to I_{SMI} needed to be performed at the j^{th} stage until all $\Lambda_{i_{SMI}}^{\Omega}(s^j)$ are evaluated. So, equation (7) can be operated at the j^{th} stage.

[0063] FIG. **8** is a simulation diagram illustrating the performance comparison of the MIMO OFDM receiver for BICM with a MMSE equalizer, the MIMO OFDM receivers for BICM with an LSD detector and a vector demapper, and the MIMO OFDM receivers for TICM as shown in FIG. **7**. The package error rate (PER) is used as the performance measure. The signal to noise ration (SNR) is defined as the average received power per receiver antenna divided by the average noise power.

$$SNR=\frac{E\{r_q'(t)\}}{\sigma^2} \quad \text{Eq. (12)}$$

where $r'_q(t)$ represents the received signal at time t at the q^{th} transmit antenna **47**.*q*.

[0064] We use an IEEE 802.11n proposal released by TGn Sync in July 2005 as our system. Note that BICM is used in the proposal. A 4×4 MIMO OFDM system with 64-QAM transmission is considered. We choose the channel-B (non-line-of-sight) with distance 6 m as our simulation environment. We also assume that frequency offset and timing offset are perfectly compensated at the receiver. The preamble for TICM is assumed to be the same with for BICM. The typical per-tone channel estimation scheme (no smoothing) is used to estimate the MIMO channels. As the standard testing, PPDU length is set as 1000 bytes, so there are 8000 information bits per package. The radius of the sphere is defined as $r_{LSD}^2=C_{LSD}\cdot N_T\cdot\sigma^2$.

[0065] We compare the performance of the system with BICM (**81**-**83**) and with TICM (**84**-**86**). For BICM, two receivers are considered; one with a MMSE equalizer and a 1-D soft-bit demapper (BICM-EQL **81**), the other with an LSD detector and a vector demapper (BICM-LSD **82**-**83**). Observing FIG. **8**, we can find that BICM-EQL **81** performs far worse than BICM-LSD **82**-**83** and TICM-LSD **84**-**86**. Also, there is about 3 dB improvement for TICM-LSD **84**-**86** compared with BICM-LSD **82**-**83**.

[0066] In addition, we compare the computational complexity of the systems with BICM and with TICM according to the number of required multiplications for the LSD detector. TABLE 1 shows the average number of required multiplications for four systems—BICM with complex-valued LSD for $C_{LSD}=16$, BICM with real-valued LSD for $C_{LSD}=16$, TICM with complex-valued LSD for $C_{LSD}=32$ and $C_{SMI}=4$, and TICM with complex-valued LSD for $C_{LSD}=32$ and $C_{SMI}=8$ at each stage.

TABLE 1

	BICM with complex-valued LSD for $C_{LSD} = 16$	BICM with real-valued LSD for $C_{LSD} = 16$	TICM with complex-valued LSD for $C_{LSD} = 32$ and $C_{SMI} = 4$	TICM with complex-valued LSD for $C_{LSD} = 32$ and $C_{SMI} = 8$
SNR = 27 (dB)	1.80E+05	4.71E+04	2.44E+03	4.79E+03
SNR = 30 (dB)	5.45E+04	1.08E+04	1.19E+03	2.30E+03
SNR = 33 (dB)	1.67E+04	3.08E+03	0.68E+03	1.28E+03

Referring to TABLE 1 and FIG. **8**, we can see that the average number of multiplications for BICM with real-valued LSD is lesser than that with complex-valued LSD. Note that the sphere of the LSD detector in TICM needs to be larger than that in BICM. So, let C_{LSD} for TICM be twice of C_{LSD} for BICM. We also can see that the average number of multiplication for TICM with C_{SMI}=8 ranges from 0.25 and 0.1 of that for BICM with real-valued LSD for PER=0.1 to PER=0.001.

[0067] In summary, the MIMO OFDM system for TICM uses a block of N_T symbols as its basic unit for interleaving. This results in different decoding architectures at the receiver. The main advantage of TICM is to merge soft-bit demapping into the Viterbi algorithm. Taking the advantage of the trellis structure inherent in the Viterbi algorithm, TICM can have lower computational complexity and potentially better performance than BICM with the LSD detector and the vector demapper. To further reduce the complexity of TICM, we make some simplifications and extend the use of the LSD algorithm in the decoding process. Although the tone-level interleaving may not have spatial diversity gain, the performance is not affected in 802.11n environments.

[0068] It will be apparent to those skilled in the art that various modifications and variations can be made to the structure of the present invention without departing from the scope or spirit of the invention. In view of the foregoing, it is intended that the present invention cover modifications and variations of this invention provided they fall within the scope of the following claims and their equivalents.

I claim:

1. A MIMO OFDM system employing N_T transmit antennas and N_R receive antennas for data transmission, the MIMO OFDM system comprising:

a transmitter, comprising:

a channel encoder for receiving information bits and outputting coded bits;

a constellation mapper for converting the coded bits into constellation symbols according to constellation mappings;

a tone-level interleaver for receiving the constellation symbols and using a symbol block of N_T constellation symbols as its basic unit for interleaving;

a parser for parsing interleaved symbol blocks and outputting parsed signals to each corresponding transmit antenna; and

multicarrier modulators for modulating the parsed signals before the parsed signals are transmitted through the corresponding transmit antennas; and

a receiver, comprising:

multicarrier demodulators for demodulating received signals passed through a MIMO channel formed by the transmit and receive antennas;

a tone-level deinterleaver for deinterleaving the received signals after demodulation, and outputting deinterleaved symbol blocks; and

a channel decoder for decoding the deinterleaved symbol blocks.

2. The MIMO OFDM system according to claim **1**, wherein the channel encoder is a conventional code (CC) encoder, and the channel decoder is a Viterbi decoder.

3. The MIMO OFDM system according to claim **1**, wherein the constellation mapper is a QAM mapper, and the constellation demapper is a QAM demapper.

4. The MIMO OFDM system according to claim **2**, wherein the Viterbi decoder comprises:

a branch metrics calculation unit for calculating branch metrics according to the deinterleaved symbol blocks and the estimated MIMO channel;

an add-compare-select (ACS) unit for performing an ACS operation according to the branch metrics; and

a survivor path decoding unit for decoding a survived path with maximum likelihood provided by the ACS operation.

5. The MIMO OFDM system according to claim **2**, wherein the Viterbi decoder comprises:

a suboptimal branch metrics calculation unit for calculating branch metrics belonging to paths beginning from the subset of beginning states with the greatest state metrics according to the deinterleaved symbol blocks and the estimated MIMO channel;

an add-compare-select (ACS) unit for performing an ACS operation according to the branch metrics; and

a survivor path decoding unit for decoding a survived path with maximum likelihood provided by the ACS operation.

6. The MIMO OFDM system according to claim **2**, wherein the Viterbi decoder comprises:

an LSD unit for using LSD algorithm to obtain a candidate path list including candidate paths;

a suboptimal branch metrics calculation unit for calculating branch metrics belonging to paths beginning from the subset of beginning states with the greatest state metrics within the candidate path list according to the deinterleaved symbol blocks and the estimated MIMO channel;

an add-compare-select (ACS) unit for performing an ACS operation according to the branch metrics; and

a survivor path decoding unit for decoding a survived path with maximum likelihood provided by the ACS operation.

7. The MIMO OFDM system according to claim **2**, further comprising:

an LSD unit for using LSD algorithm to obtain a candidate path list including candidate paths;

a branch metrics calculation unit for calculating branch metrics belonging to paths within the candidate path list according to the deinterleaved symbol blocks and the estimated MIMO channel;

an add-compare-select (ACS) unit for performing an ACS operation according to the branch metrics; and

a survivor path decoding unit for decoding a survived path with maximum likelihood provided by the ACS operation.

8. A MIMO OFDM receiver for a MIMO OFDM system employing N_T transmit antennas and N_R receive antennas for data transmission, the MIMO OFDM receiver comprising:

multicarrier demodulators for demodulating received signals passed through a MIMO channel formed by the transmit and receive antennas, wherein the received signals are interleaved by using a symbol block of N_T constellation symbols as its basic unit;

a tone-level deinterleaver for deinterleaving the received signals after demodulation, and outputting deinterleaved symbol blocks; and

a channel decoder for decoding the deinterleaved symbol blocks.

9. The MIMO OFDM receiver according to claim **8**, wherein the channel decoder is a Viterbi decoder.

10. The MIMO OFDM receiver according to claim **8**, wherein the constellation demapper is a QAM demapper.

11. The MIMO OFDM receiver according to claim **9**, wherein the Viterbi decoder comprises:

a branch metrics calculation unit for calculating branch metrics according to the deinterleaved symbol blocks and the estimated MIMO channel;

an add-compare-select (ACS) unit for performing an ACS operation according to the branch metrics; and

a survivor path decoding unit for decoding a survived path with maximum likelihood provided by the ACS operation.

12. The MIMO OFDM receiver according to claim **9**, wherein the Viterbi decoder comprises:

a suboptimal branch metrics calculation unit for calculating branch metrics belonging to paths beginning from the subset of beginning states with the greatest state metrics according to the deinterleaved symbol blocks and the estimated MIMO channel;

an add-compare-select (ACS) unit for performing an ACS operation according to the branch metrics; and

a survivor path decoding unit for decoding a survived path with maximum likelihood provided by the ACS operation.

13. The MIMO OFDM receiver according to claim **9**, wherein the Viterbi decoder comprises:

an LSD unit for using LSD algorithm to obtain a candidate path list including candidate paths;

a suboptimal branch metrics calculation unit for calculating branch metrics belonging to paths beginning from the subset of beginning states with the greatest state metrics within the candidate path list according to the deinterleaved symbol blocks and the estimated MIMO channel;

an add-compare-select (ACS) unit for performing an ACS operation according to the branch metrics; and

a survivor path decoding unit for decoding a survived path with maximum likelihood provided by the ACS operation.

14. The MIMO OFDM receiver according to claim **9**, further comprising:

an LSD unit for using LSD algorithm to obtain a candidate path list including candidate paths;

a branch metrics calculation unit for calculating branch metrics belonging to paths within the candidate path list according to the deinterleaved symbol blocks and the estimated MIMO channel;

an add-compare-select (ACS) unit for performing an ACS operation according to the branch metrics; and

a survivor path decoding unit for decoding a survived path with maximum likelihood provided by the ACS operation.

* * * * *